https://doi.org/10.5194/egusphere-2025-3925
Preprint. Discussion started: 26 August 2025

Potential of various minerals and their biogeochemical implications for ocean alkalinity enhancement in the southeastern Arabian Sea

Shreya Mehta[1,2], Jitender Kumar[1], Sipai Nazirahmed[1], Himanshu Saxena[1], Jyotiranjan S. Ray[1], Sanjeev Kumar[1], Indrani Karunasagar[3], and Arvind Singh[1]

[1]Physical Research Laboratory, Ahmedabad, 380009, India
[2]Indian Institute of Technology, Gandhinagar, 382355, India
[3]NITTE University, Mangalore, 575018, India

Correspondence: Arvind Singh (arvinds@prl.res.in)

Abstract. Ocean alkalinity enhancement (OAE) is emerging as a promising yet largely untested marine carbon dioxide (CO_2) removal approach. It involves the addition of alkaline substances such as powdered minerals and aqueous hydroxide solutions to seawater, shifting the carbonate chemistry speciation towards carbonate ions so as to store more CO_2. Contemporaneous studies are being carried out to evaluate the efficacy, durability, and risks associated with these substances. Given the heterogeneity in a natural ecosystem, each substance will have distinct implications on carbonate chemistry as well as biogeochemistry of a given ecosystem. Our study contributes to ongoing research by examining the response of the ocean's carbonate chemistry to the addition of various alkalinity feedstocks — including both naturally occurring and anthropogenically (industrially) produced minerals, along the southeastern coastal Arabian Sea. We tested the alkalinity (A_T) generation potential and traced the associated changes in the carbonate chemistry speciations for three naturally occurring minerals: (i) olivine ($(MgFe)_2SiO_4$), (ii) kaolinite ($Al_2Si_2O_5(OH)_4$), and (iii) dolomite ($CaMg(CO_3)_2$), and for two anthropogenically produced minerals: (i) periclase (MgO) and (ii) hydrated lime ($Ca(OH)_2$) of two different mineral compositions, using 300 L mesocosms. Overall, no significant changes in A_T, pH and dissolved inorganic carbon (DIC) were observed for the naturally occurring minerals, suggesting the lower efficiency of these minerals to increase A_T. In contrast, the dissolution of periclase and hydrated lime increased A_T (up to 16%, which corresponds to 80% of the total added A_T) and pH by up to 0.6 units. We further demonstrate that the temporal changes in the carbon isotopic composition ($\delta^{13}C$) of DIC as well as the changes in the DIC concentration occurring within the mesocosms can serve as an effective and reliable proxy for tracing secondary carbonate precipitation. As loss of alkalinity via secondary precipitation diminishes the overall efficiency of the OAE approach, accurate determination of the threshold at which secondary precipitation is triggered is critical for maximizing the effectiveness of this method. We determine these thresholds and provide an assessment of various alkalinity feedstocks that could work best for OAE.

1 Introduction

Since the onset of the industrial revolution, there has been a steep rise in the concentration of carbon dioxide (CO_2) in the atmosphere (from 280 ppmv in 1850 to 426 ppmv at present (Lan et al., 2025)), contributing towards global warming and, by extension, to climate change (IPCC, 2023). The ocean serves as a prominent sink of CO_2 by absorbing roughly one-fourth of

https://doi.org/10.5194/egusphere-2025-3925
Preprint. Discussion started: 26 August 2025

the anthropogenic CO_2 (Gruber et al., 2023). While this ocean sink has slowed down the extent of otherwise greater warming, it has concurrently resulted in widespread ecological consequences (Venegas et al., 2023). The uptake of excess CO_2 by the seawater increases the hydrogen ion concentration $[H^+]$, leading to a decrease in the pH of the ocean. This phenomenon, commonly known as ocean acidification, causes a substantial change in marine carbonate chemistry by lowering the calcium carbonate saturation state (Ω) in surface waters, having direct consequences for marine calcifiers (Feely et al., 2004). Climate change has already caused substantial damage to our ecosystem, and in some cases, the damage seems irreversible (IPCC, 2023). Global efforts are being made to tackle climate change, and the Paris Agreement, 2015 has been one of the milestones in this process. One of the overarching goals of this agreement is to limit human-induced global warming to below 1.5° C. However, this targeted threshold is at a risk of being surpassed in the next five to ten years (Cannon, 2025; Rohde, 2025) even if we cut emissions to zero. Thus, to limit this warming, we require strong reductions in greenhouse gas emissions coupled with the implementation of various carbon dioxide removal (CDR) methods at the global level (Minx et al., 2018; Rau et al., 2012).

Various marine CDR (mCDR) methods, e.g., ocean fertilization, macroalgae cultivation, ocean alkalinity enhancement (OAE), and artificial upwelling, have been proposed and are being assessed worldwide (Oschlies et al., 2025; Doney et al., 2025; NASEM, 2019, 2021). Currently, the ocean sequesters around one-fourth of the anthropogenic CO_2 due to its physicochemical properties (Friedlingstein et al., 2025). When CO_2 dissolves in seawater, it forms a vast reservoir of CO_2 in the form of dissolved inorganic carbon (DIC, 37000 Gt C in the ocean) (Friedlingstein et al., 2025). This vast potential of the ocean underpins its potential as an mCDR to mitigate climate change. Ocean alkalinity enhancement (OAE) is one of the mCDRs with the potential not only to sequester CO_2 but also to counteract ocean acidification by increasing the pH and Ω (Kheshgi, 1995; Feng et al., 2016; Lenton et al., 2018). If implemented on a global scale, OAE has the potential to remove >1 Gt CO_2 yr^{-1} from the atmosphere, which is more than what natural silicate weathering could achieve (Renforth and Henderson, 2017). OAE can be carried out by spreading powdered minerals, raining aqueous solutions of hydroxides (i.e., water jets containing a slurry of alkaline minerals pumped into the air from the ships), and by electrochemical alkalinity generation (Kheshgi, 1995; Hartmann et al., 2013; Renforth and Henderson, 2017; Bianchi et al., 2024). These alkalinity sources may differ in their origin, dissolution kinetics, amount of alkalinity released, and their impact on chemical speciations and biological responses. Although OAE has drawn huge attention in the past decade, there are considerable knowledge gaps and uncertainties about the risks, efficacy, durability, and sustainability of this method (Keller et al., 2014; González and Ilyina, 2016). Current global research is focused on evaluating the efficiency of various alkalinity feedstocks to identify the most effective and scalable options for large-scale OAE deployment (Hartmann et al., 2023). A diverse range of ecosystems makes it even more difficult to conduct a comprehensive assessment of potential risks, highlighting the need for community efforts to build a standardized framework for environmental evaluation (Bach, 2024).

While it is imperative to discuss the consequences of mineral addition, the foremost task is to identify the mineral(s) with significant potential for OAE (Guo et al., 2025a), followed by constraining the amount to be added to attain a stable alkalinity and preventing any secondary precipitation (Moras et al., 2022; Hartmann et al., 2023; Suitner et al., 2024). Elevated alkalinity levels can result in secondary precipitation, which decreases the CDR potential of OAE and, in some cases, causes net loss of

https://doi.org/10.5194/egusphere-2025-3925
Preprint. Discussion started: 26 August 2025

alkalinity through runaway precipitation (Moras et al., 2022; Hartmann et al., 2023). So far, small-scale laboratory experiments have been carried out to determine the critical or safe threshold for alkalinity addition (Moras et al., 2022; Hartmann et al., 2023; Suitner et al., 2024), but given the complexity and heterogeneity of natural ecosystems, these studies are insufficient to validate the consequences of deploying OAE in real-world diverse ecosystems. Modelling studies are also being carried out to provide an assessment of OAE on a global scale and associated long-term changes in ocean biogeochemistry (Ilyina et al., 2013; Burt et al., 2021), but these studies are often associated with large uncertainties mainly attributed to the lack of observational data.

Mesocosm experiments offer a more realistic replication of natural environmental conditions and can be sustained for a longer period of time (Riebesell et al., 2023). Majority of the existing mesocosm studies are restricted to the regions in the North Atlantic Ocean with alkalinity sources being alkaline liquids such as NaOH (Paul et al., 2025; Ferderer et al., 2024; Marín-Samper et al., 2024; Suessle et al., 2025). Previous studies have identified coastal regions as the most viable site for CDR deployment, as near-coast operations are economically favourable from a resource perspective (Renforth and Henderson, 2017; He and Tyka, 2023). Considering the vast expanse of the northern Indian Ocean and the extensive Indian coastline ($\sim 11 \times 10^3$ km), this region may emerge as a promising candidate for large-scale CDR deployment in the future scenario.

Here we present a mesocosm experiment designed to investigate the following (i) the alkalinity generation potential of naturally occurring minerals (olivine, kaolinite and dolomite) and anthropogenically produced minerals (periclase and hydrated lime) in the coastal water of the southeastern Arabian Sea (ii) define the threshold of alkalinity addition so as to prevent secondary precipitation and (iii) effect of mineral addition on various biogeochemical processes.

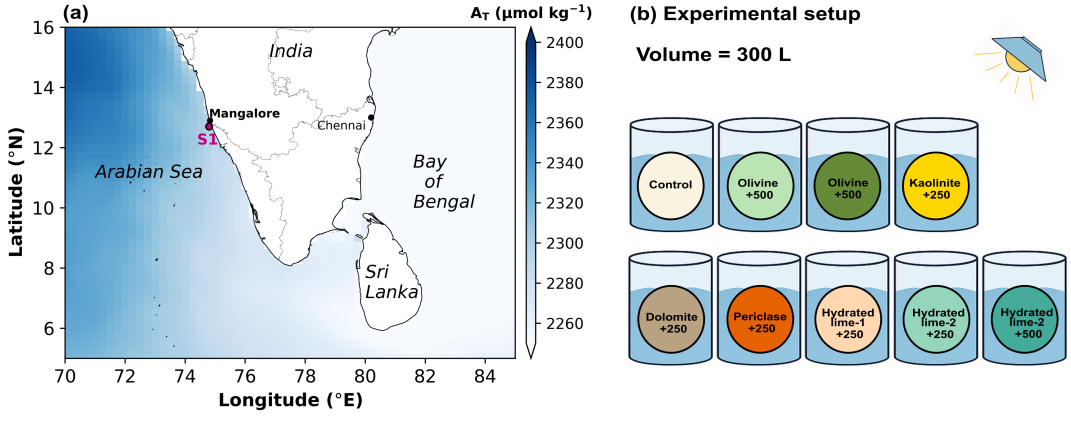

Figure 1. Study area and mesocosm experimental setup. (a) Location in the coastal Arabian Sea (site S1) where seawater was collected for the mesocosm experiment conducted at NITTE University, Mangalore. The background colour shows the variability in the total alkalinity in the surface ocean generated using E.U. Copernicus Marine Service Information (https://doi.org/10.48670/moi-00015). (b) Each mesocosm is represented by a tank filled with water up to 300 L, with details of the minerals added and the targeted alkalinity increase of +250 or +500 μmol kg^{-1}. One of the mesocosms served as a control with no mineral addition. Each mesocosm was also provided with an artificial light source to mimic the natural day and night cycle.

https://doi.org/10.5194/egusphere-2025-3925
Preprint. Discussion started: 26 August 2025

Table 1. Summary of sampling approach, measured parameters, and timing of sample collection before and after mineral addition during the mesocosm experiment carried out over nine days.

		Before mineral addition	After mineral addition												
	Day	1	1	1	1	2	2	2	3	3	3	4	5	7	9
	Date (dd.mm.yy)	17.11.22	17.11.22	17.11.22	17.11.22	18.11.22	18.11.22	18.11.22	19.11.22	19.11.22	19.11.22	20.11.22	21.11.22	23.11.22	25.11.22
	Time (hrs)	09:00	10:30	16:30	20:30	09:30	13:30	17:30	09:30	13:40	17:30	09:30	09:30	09:30	09:30
Parameters	Temperature	✓	✓	✓	✓	✓	✓	✓	✓	✓	✓	✓	✓	✓	✓
	pH	✓	✓	✓	✓	✓	✓	✓	✓	✓	✓	✓	✓	✓	✓
	Salinity	✓	✓	✓	✓	✓	✓	✓	✓	✓	✓	✓	✓	✓	✓
	DIC	✓	✓	✓	✓	✓	✓	✓	✓	✓	✓	✓	✓	✓	✓
	Alkalinity	✓	✓	✓	✓	✓	✓	✓	✓	✓	✓	✓	✓	✓	✓
	$\delta^{13}C_{DIC}$	✓	✓	✓	✓	✓	✓	✓	✓	✓	✓	✓	✓	✓	✓

DIC: dissolved inorganic carbon

2 Materials and methods

2.1 Study area and experimental setup

We collected seawater from a nearshore site in the southeastern Arabian Sea, near Mangalore, India (12°47'48.1" N, 74°50'45.9" E) (Fig. 1 (a)). The seawater was transported to an indoor mesocosm facility at NITTE University, Mangalore, Karnataka, India. The nine mesocosms were filled with up to 300 L of seawater, one was kept as a control, while the remaining eight were doped with different industrial-grade minerals and monitored and maintained for nine days (from 17 to 25 November 2025) (Fig. 1 (b)). The minerals included were olivine, kaolinite, dolomite, periclase, and two distinct compositions of hydrated lime: hydrated lime-1 (70% $Ca(OH)_2$) and hydrated lime-2 (54% $Ca(OH)_2$), with a grain size of ≤ 63 μm. Alkalinity enhancement was targeted at two A_T levels (+A_T); 250 μmol kg^{-1} in four mesocosm using olivine, kaolinite, dolomite, hydrated lime-2 and +A_T of 500 μmol kg^{-1} in the remaining four mesocosms using olivine, periclase, hydrated lime-1 and hydrated lime-2. All mesocosms were equipped with artificial light sources (LED white lights) with a light intensity of $\sim$194 μmol m^{-2} s^{-1}, and operated to mimic the natural diel cycle (10:14 h light: dark period). Each mesocosm was tracked for changes in carbonate chemistry along with changes in biogeochemical processes. The details of sampling for all the parameters are provided in Table 1.

2.2 Analytical methods

The chemical composition of the minerals was analysed using X-ray fluorescence spectrometry (XRF), while the mineral phases were identified using X-ray diffraction (XRD). The detailed description of the XRF and XRD analysis is provided in the Supplementary Information (Text S1). Quantitative analysis was carried out using Rietveld Refinement to identify the proportion of different mineral phases within the bulk powder using Profex 5.4. Temperature, salinity, and pH were measured in situ using a multi-parameter meter (Hanna®). The pH electrode was calibrated using three buffer solutions of pH 4.01, 7.01, and 10.01, corresponding to a pH measurement on the NIST scale. The water samples for A_T were filtered through 0.2 μm nylon filter, collected in 60 mL HDPE amber bottles without leaving any headspace and stored at 4°C under dark conditions.

https://doi.org/10.5194/egusphere-2025-3925
Preprint. Discussion started: 26 August 2025

The A_T was determined by open cell dynamic end-point titration method with 0.05 N HCl solution prepared in 0.7 N NaCl solution and calibrated with Na_2CO_3 standard solutions (ranging from 1900 - 3000 μmol kg^{-1}) using an automated titration system (Metrohm, 916 Ti-Touch) with 10 mL dosing unit (Metrohm 800 Dosino) and a combined glass electrode (Dickson et al., 2007). In addition to the mineral addition, physical processes like evaporation also control the A_T. Since the mesocosms were open to the atmosphere, the evaporation contributed to an increase in the alkalinity. Assuming that evaporation affects both salinity and A_T similarly, we corrected the alkalinity measurements for evaporation by normalizing them to the salinity of the control as:

$$A_{T\text{norm}} = \left(\frac{A_{Tm}(t)}{S_c(t)}\right) \cdot S_c(0) \quad (1)$$

where $A_{T\text{norm}}$ is the alkalinity normalized to evaporation, $A_{Tm}(t)$ is the alkalinity of the mesocosms to which minerals were added at time *t*, $S_c(t)$ is the salinity of the control at time *t*, and $S_c(0)$ is the salinity of the control at time *t* = 0 (i.e., before mineral addition). Hereafter, A_T denotes the $A_{T\text{norm}}$ for all the mesocosms .

The samples for DIC measurements were collected in glass serum bottles without leaving headspace and poisoned with 0.2 mL supersaturated $HgCl_2$ solution. The DIC and $\delta^{13}C_{DIC}$ were determined using the GAS-Bench coupled to an Isotope Ratio Mass Spectrometer (IRMS, MAT 253). The instrument was calibrated with Na_2CO_3 standard solutions (1000 - 4000 μmol kg^{-1} Na_2CO_3). DIC concentrations were measured with a precision better than 4 %. The $\delta^{13}C_{DIC}$ values are reported within the standard deviation of less than 0.1 ‰.

Carbonate chemistry speciations were calculated using the CO2SYS python program (version 1.8.2) (Humphreys et al., 2022) based on the measured pH and A_T. We used the boric acid dissociation constant, the carbonic acid dissociation constant, and the sulphuric acid dissociation constant from Uppström (1974), Lueker et al. (2000), and Dickson (1990), respectively, for deriving the carbonate chemistry speciation.

2.3 Statistical analyses

For statistical analyses, we fitted the Generalised Additive Models (GAMs) from the "mgcv" package in R Studio (R version 4.5.1) following Simpson (2017) and Guo et al. (2024). GAMs are used to detect significant changes in the mean and trend of different treatment groups with control and within the treatment groups through time. We used the following GAM equation:

$$Y = \text{Treatment} + s(\text{Days}) + s(\text{Days, by = oTreatement}) \quad (2)$$

where "Y" is the dependent variable, "Treatment" represents the parametric factor, s(Days) is the smooth function for reference group (control or any other treatment) and s(Day, by = oTreatment) is the non-parametric smoothening factor that allows fitting of smooth time trends for each group, and captures the difference in the treatment and the reference group. When comparing the mean values of two groups, the term "*P*-means" represents the *p* value, and if it is <0.5, it indicates that the mean value of the treatment group is significantly different from the reference group. Similarly, "*P*-smooths" represents the *p* value for the smooth term in the GAMs. If *P*-smooths is <0.5, it indicates that there is a significant difference in the trend of the two

https://doi.org/10.5194/egusphere-2025-3925
Preprint. Discussion started: 26 August 2025

groups. Hereafter, the "significant" term refers exclusively to the statistical significance (p value <0.5). The summary of the GAM analysis is provided in Table S1.

3 Results

3.1 Mineral composition

The weight % (wt %) oxides for all the added minerals are summarized in Table 2, and the XRD profiles for all the mineral powders are provided in Supplementary Information Fig. S1. The XRD analysis determined the mineral phases as well as the relative proportion of different mineral phases. Powdered olivine mineral predominantly consisted of forsterite (90 %) with a minor fraction of fayalite (10 %). Kaolinite, dolomite, and periclase were determined to be nearly pure phases. The hydrated lime had a variable amount of $CaCO_3$ present. Hydrated lime-1 comprised of 70 % $Ca(OH)_2$ and 30 % $CaCO_3$ whereas hydrated lime-2 comprised of almost equal proportion of $Ca(OH)_2$ (54 %) and $CaCO_3$ (46 %). This difference in the composition can be attributed to incomplete calcination of raw material or the carbonation of CaO to $CaCO_3$ during the formation of $Ca(OH)_2$.

Table 2. Major oxide concentrations (normalized to 100 %) in the added minerals obtained from the XRF analysis.

	SiO_2 (wt %)	Al_2O_3 (wt %)	Fe_2O_3 (wt %)	MgO (wt %)	CaO (wt %)
Olivine	42.7	bdl	15.1	41.4	0.5
Kaolinite	44.1	50.4	1.5	0.8	0.8
Dolomite	14.5	0.3	1.3	27.9	55.9
Periclase	2.5	0.3	0.8	95.2	1.1
Hydrated lime-1	3.5	bdl	1.1	2.1	93.0
Hydrated lime-2	2.0	1.0	1.0	1.9	93.9

bdl: below detection limit

3.2 Variation in A_T, pH and DIC

The initial A_T, pH and DIC of the seawater were ~2298 μmol kg^{-1}, 7.71 units and ~2137 μmol kg^{-1}, respectively, representing the carbonate chemistry prior to mineral addition. Overall, we observed no increase in the A_T over nine days for the kaolinite$_{(+250)}$, olivine$_{(+250),(+500)}$ and dolomite$_{(+250)}$ treatments (Fig. 2 (a) and (c)) (P-means and P-smooths <0.05). The GAMs for all the treatments compared to the control showed significant differences in the mean pH (P-means <0.05). An increase in A_T was observed in the case of periclase$_{(+500)}$, hydrated lime-1$_{(+250)}$, hydrated lime-2$_{(+250)}$ and hydrated lime-2$_{(+500)}$. The periclase$_{(+500)}$ addition increased the A_T by ~360 μmol kg^{-1} (ΔA_T: difference between final A_T and initial (before A_T addition)) within 1.5 hours of mineral addition (Fig. 2 (b) and (d)) and overall trend was also significantly different from control (P-smooths <0.05). The increase in A_T for periclase$_{(+500)}$ was also accompanied by a rise in pH from 7.7 to 8.1 after the mineral addition (Fig. 2 (f)). For hydrated lime-1$_{(+250)}$ the A_T increased by ~190 μmol kg^{-1} and pH by ~0.2 units within 1.5 hours of mineral addition. For hydrated lime-2$_{(+250)}$ and hydrated lime-2$_{(+500)}$ the alkalinity increased by ~120

https://doi.org/10.5194/egusphere-2025-3925
Preprint. Discussion started: 26 August 2025

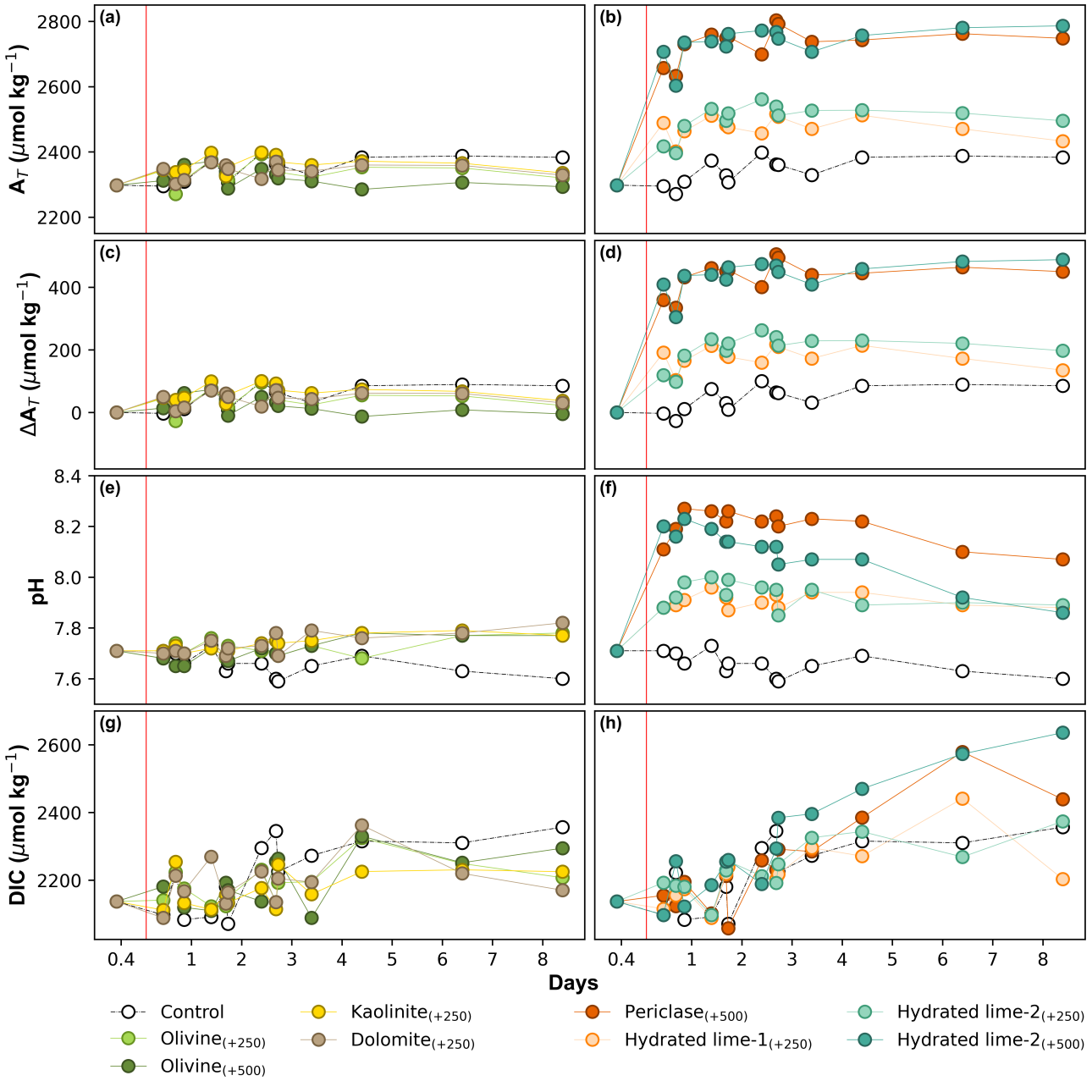

Figure 2. Trends in total alkalinity (A_T) ((a),(b)), change in total alkalinity (ΔA_T) ((c),(d)), pH ((e),(f)) and dissolved inorganic carbon (DIC) ((g),(h)) following addition of naturally occurring minerals (left panel) and anthropogenic minerals (right panel) in mesocosms over a period of nine days. The A_T is the normalized (corrected for the effect of evaporation) total alkalinity. The vertical red line marks the time of mineral addition.

https://doi.org/10.5194/egusphere-2025-3925
Preprint. Discussion started: 26 August 2025

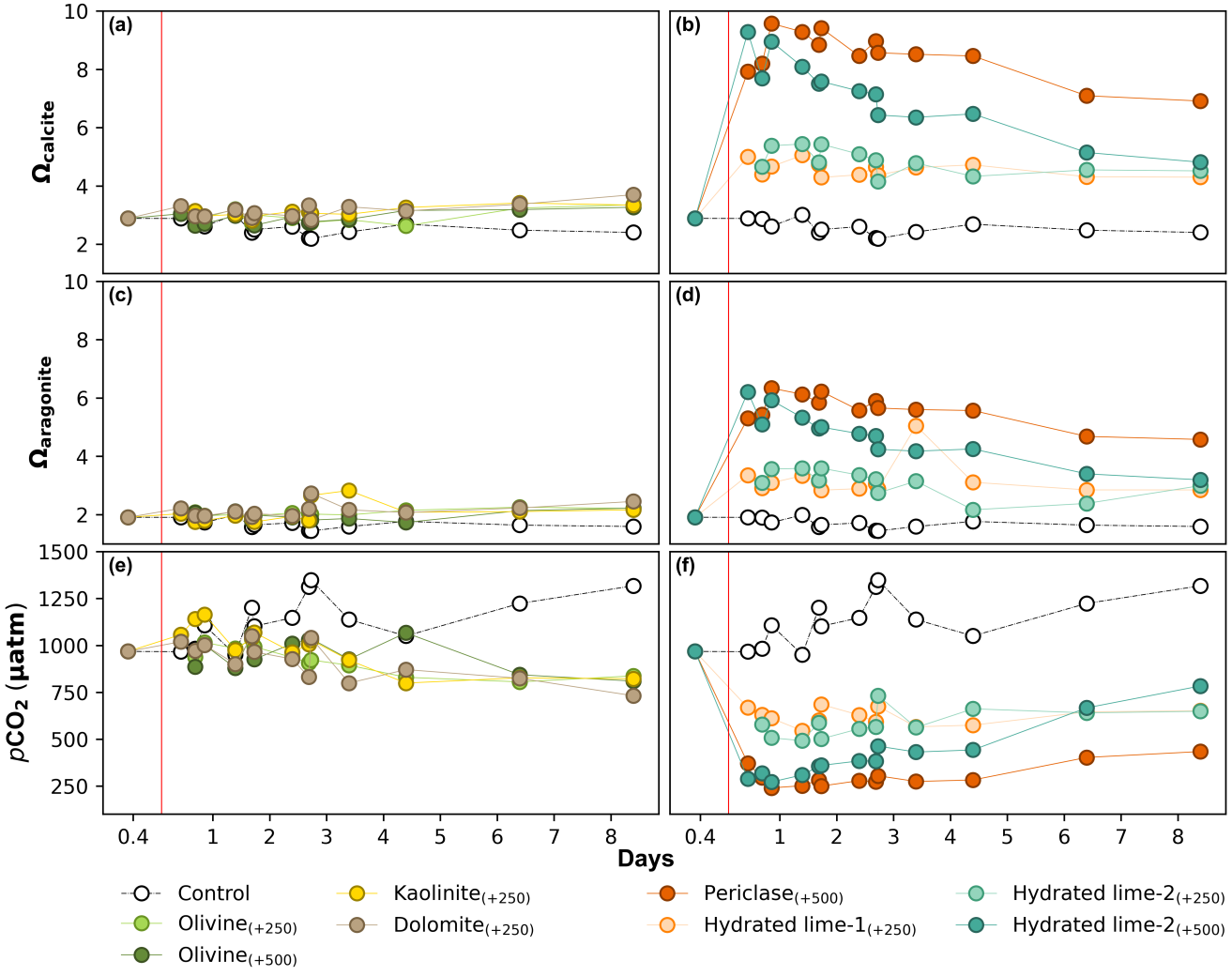

Figure 3. Temporal changes in calcite saturation state ($\Omega_{calcite}$) ((a),(b)), aragonite saturation state ($\Omega_{aragonite}$) ((c),(d)) and partial pressure of CO_2 in seawater (pCO_2) ((e),(f)), following dissolution of naturally occurring minerals (left panel) and anthropogenic minerals (right panel) in seawater over a period of nine days. The vertical red line marks the time of mineral addition.

and ∼400 μmol kg^{-1}, respectively, (Fig. 2 (b) and (d)) and the pH increased by ∼0.2 and ∼0.5 units, respectively, (Fig. 2 (f)) within 1.5 hours of mineral addition. The mean DIC concentrations were higher for only hydrated lime-2$_{(+500)}$ (*P*-means and
155 *P*-means <0.05) (Fig. 2 (h)). We also compared two olivine treatments (olivine$_{(+250)}$ and olivine$_{(+500)}$) with each other and found no significant difference in A_T, pH and DIC over time (*P*-means and *P*-smooths >0.05). Contrary to this, A_T, pH and DIC of hydrated lime-2$_{(+250)}$ and hydrated lime-2$_{(+500)}$ were significantly different from each other (*P*-means and *P*-smooths <0.05).

https://doi.org/10.5194/egusphere-2025-3925
Preprint. Discussion started: 26 August 2025

3.3 Variation in $\Omega_{calcite}$, $\Omega_{aragonite}$ and pCO_2

The saturation states of calcite ($\Omega_{calcite}$) and aragonite ($\Omega_{aragonite}$), and the partial pressure of CO_2 (pCO_2) of seawater prior to mineral addition were 3 units and 2 units, and 970 μatm, respectively. The $\Omega_{calcite}$, and $\Omega_{aragonite}$ increased for kaolinite$_{(+250)}$, dolomite$_{(+250)}$, periclase$_{(+500)}$, hydrated lime-1$_{(+250)}$, hydrated lime-2$_{(+250)}$ and hydrated lime-2$_{(+500)}$ (Fig. 3 (a), (b), (c) and (d)). The overall trend of $\Omega_{calcite}$, and $\Omega_{aragonite}$ was different from control only for periclase$_{(+500)}$ and hydrated lime-2$_{(+500)}$ (*P*-smooths <0.05). For periclase$_{(+500)}$, the $\Omega_{calcite}$ and $\Omega_{aragonite}$ reached ~10 and ~6, respectively, within 12 hours of mineral addition (Fig. 3 (b) and (d)) and dropped to ~7 and ~5, respectively, on the ninth day. For both hydrated lime-1$_{(+250)}$ and hydrated lime-2$_{(+250)}$, the $\Omega_{calcite}$ and $\Omega_{aragonite}$ increased to ~5 and ~3.5, respectively, within 12 hours of mineral addition (Fig. 3 (b) and (d)). In case of hydrated lime-2$_{(+500)}$, $\Omega_{calcite}$ and $\Omega_{aragonite}$ rapidly increased to ~9 and ~6, respectively, within 1.5 hours of mineral addition, however, both the saturation states began to decline over time reaching ~5 and ~3 at the end of the experiment (Fig. 3 (b) and (d)). Overall, the pCO_2 decreased in all the treatments (*P*-means and *P*-smooths <0.05) (Fig. 3 (e) and (f)). The pCO_2 for periclase$_{(+500)}$ dropped by ~600 μatm within 1.5 hours of mineral addition and by ~700 μatm within 12 hours of mineral addition (Fig. 3 (f)). For both hydrated lime-1$_{(+250)}$ and hydrated lime-2$_{(+250)}$ pCO_2 fell by 420 and 470 μatm within 12 hours of mineral addition (Fig. 3 (f)). The pCO_2 dropped by ~700 μatm for hydrated lime $_{(+500)}$ by the end of day first day (Fig. 3 (f)). No significant difference for $\Omega_{calcite}$, $\Omega_{aragonite}$ and pCO_2 was observed between olivine$_{(+250)}$ and olivine$_{(+500)}$ (*P*-means and *P*-smooths >0.05). However, $\Omega_{calcite}$, $\Omega_{aragonite}$ and pCO_2 differed notably between the hydrated lime-2$_{(+250)}$ and hydrated lime-2$_{(+500)}$ (*P*-means and *P*-smooths <0.05).

4 Discussion

4.1 Potential of natural and artificial minerals to enhance ocean alkalinity

The present study attempts to explore the potential of the Indian coast for mineral-based OAE using a mesocosm experiment. Over the nine days, variation in A_T, pH and DIC were monitored. For the added natural minerals - kaolinite, dolomite and olivine, overall we observed no change in the A_T (Fig. S2). However, dissolution of minerals such as periclase and hydrated lime occurred rapidly, causing a steep rise in A_T as well as the pH (Fig. 2 (b), (d), (f) and (h)). The mean effect of the alkalinity released by these minerals was higher than that of the control mesocosm (Fig. S2). Renforth and Henderson (2017) have summarised the dissolution kinetics of various natural and anthropogenic minerals and, as expected, our results demonstrate that compared to the chosen natural minerals, anthropogenically produced minerals dissolves more rapidly and have a more pronounced effect on the A_T and pH (Fig. 2 (b), (d) and (f)). The increase in A_T and pH is accompanied by a decrease in the pCO_2 levels in periclase and hydrated lime treatments (Fig. 2 (h)). As the pH increases, the carbonate equilibrium shifts towards the HCO_3^- and CO_3^{2-}, causing an increase in saturation state. Seawater is often saturated with respect to $CaCO_3$, and supersaturation beyond a certain threshold triggers secondary precipitation of inorganic calcium carbonate (in the form of calcite or aragonite), resulting in loss of A_T and pH due to mineral addition (Takahashi et al., 2014; Koishi, 2017). However, in our experiment, for hydrated lime-1,2$_{(+250)}$, hydrated lime-2$_{(+500)}$ and periclase$_{(+500)}$, we observed that there was

https://doi.org/10.5194/egusphere-2025-3925
Preprint. Discussion started: 26 August 2025

no decline in A_T and pH with time, thus eliminating the possibility of secondary precipitation. Overall, consistently high pH trend over nine days for periclase and hydrated lime highlights the potential of these minerals to contribute to tackle the ocean acidification. The A_T and pH-driven saturation states suggest that secondary precipitation may not occur in the study area, i.e. the southeastern Arabian Sea, even at $\Omega_{calcite}$ ~10 and $\Omega_{aragonite}$ ~6. This further implies that the A_T addition levels of 500 μmol kg^{-1} and below for both periclase and hydrated lime can be considered optimal thresholds for this region.

While the concept of OAE stems from the long-term weathering of basaltic rocks, it is believed that mafic or ultramafic rocks are viable candidates for OAE due to their high weatherability, (Geerts et al., 2025b). The use of pure minerals such as olivine and pyroxenes would be more effective, as these minerals are relatively unstable and highly susceptible to weathering when exposed to near-surface environmental conditions (Schuiling and Krijgsman, 2006). Modelling studies suggest that olivine has a high potential towards CO_2 sequestration in the coastal regions, but the time frame in which it dissolves is largely dependent on the physical properties of seawater (e.g., temperature and pH) as well as the grain size of the mineral (Ramasamy et al., 2024; Geerts et al., 2025a). Small-scale laboratory experiments concluded that olivine dissolution causes a significant increase in the A_T followed by an increase in DIC, but are sceptical about its efficiency in field trials (Montserrat et al., 2017). Contrary to these studies Guo et al. (2024) through a microcosm experiment in the coastal waters of Tasmania have shown that the dissolution of olivine has limited potential for CDR at smaller time scales, but its environmental impacts are more pronounced. In line with the microcosm experiment, our mesocosm experiment showed no change in A_T for both the targeted alkalinity levels of olivine$_{(+250,+500)}$. Additionally, there was no significant difference in A_T between the two added alkalinity levels for olivine$_{(+250,+500)}$, suggesting the limited potential of olivine for OAE in this region. Although the theoretical CO_2 removal efficacy of olivine is high, its limited dissolution in natural settings questions its practical effectiveness. Studies have shown that calcium-based products such as steel slag, CaO and $Ca(OH)_2$ release significant A_T, thereby exhibiting a higher potential for CDR (Guo et al., 2024; de Castro et al., 2025). Researchers for a long time have questioned the techno-economic feasibility of these minerals and have been skeptical about costs associated with the raw materials and processing (Kheshgi, 1995; Hartmann et al., 2013). However, given the potential of these minerals for OAE, they are being reconsidered and revaluated as potential OAE methods (Foteinis et al., 2022). Building on this as well as findings of our study, we suggest that it is essential to explore and identify the effective and promising solutions, including the industrially derived minerals as well as their by-products.

4.2 Tracing biogeochemical processes using DIC concentration and $\delta^{13}C_{DIC}$

Isotopic fractionation occurring during various physico-chemical processes governs the carbon isotope composition ($\delta^{13}C$) of DIC ($\delta^{13}C_{DIC}$) in seawater (Fig. 4 (a)). The dominant processes that regulate $\delta^{13}C_{DIC}$ are primary production/photosynthesis, CO_2 outgassing, calcium carbonate precipitation, dissolution of calcium carbonate and remineralisation/respiration of organic matter. Preferential uptake of ^{12}C into biomass during photosynthesis leads to an enrichment of ^{13}C in the remaining pool of DIC. Photosynthesis drives increased uptake of HCO_3^-, leading to a simultaneous decrease in the DIC concentration. In contrast, remineralisation of the organic matter facilitates the preferential release of the lighter isotopic signatures (^{12}C) into the seawater, making the DIC pool depleted in ^{13}C and simultaneously increasing the overall DIC concentration. Likewise,

https://doi.org/10.5194/egusphere-2025-3925
Preprint. Discussion started: 26 August 2025

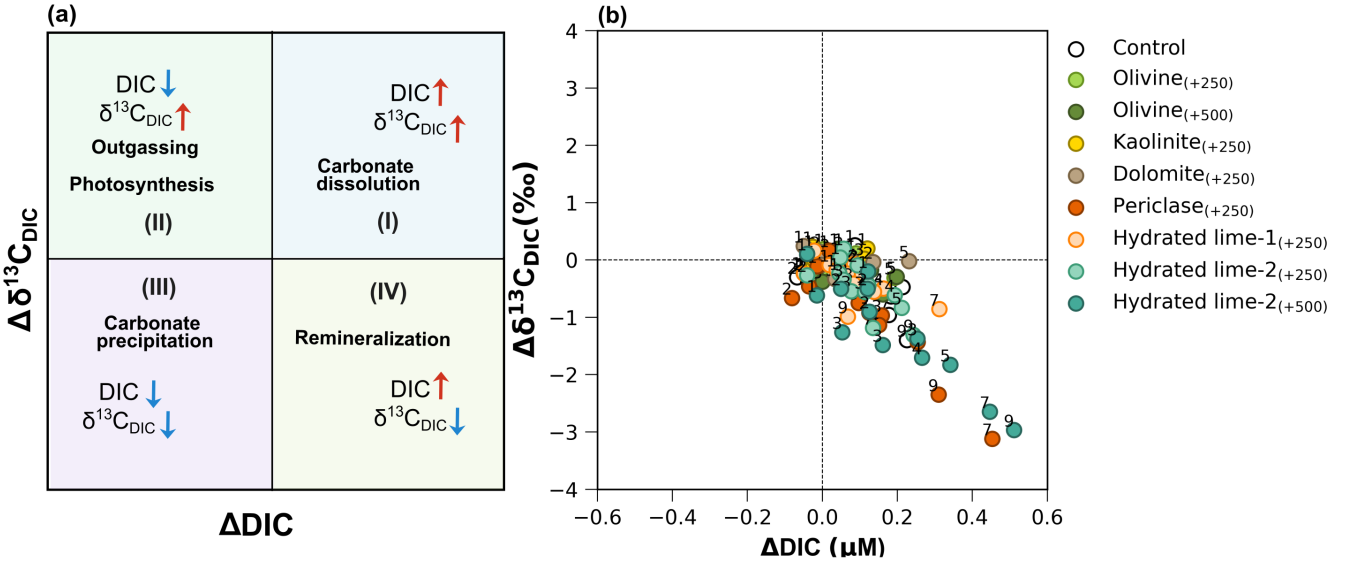

Figure 4. (a) Variation in the carbon isotopic composition (δ^{13}C) of dissolved inorganic carbon (DIC) and DIC due to various biogeochemical processes. The red arrow indicates an increase and the blue arrow indicates a decrease in the DIC and $\delta^{13}C_{DIC}$ due to these processes. (b) The change in DIC (ΔDIC) plotted against the change in $\delta^{13}C_{DIC}$ ($\Delta\delta^{13}C_{DIC}$) for all the treatments. The number associated with each data point refers to the respective sampling days (1-9).

the carbonate dynamics also influence the isotopic composition and concentration of DIC. Carbonate dissolution enriches the DIC pool in ^{13}C, resulting in higher $\delta^{13}C_{DIC}$ values, whereas carbonate precipitation depletes the DIC in ^{13}C, resulting in low $\delta^{13}C_{DIC}$ values. The dissolution and precipitation of carbonates tend to increase and decrease the DIC concentration, respectively. Since mesocosms are isolated system with no external inputs that could alter the isotopic composition, monitoring the temporal changes in the carbon isotopic composition in the DIC along with the DIC concentration within the mesocosms provides insights to identify the dominant process occurring within the mesocosms. Figure 4 (b) illustrates the change in the DIC concentration with respect to the initial value (ΔDIC), plotted against the change in the $\delta^{13}C_{DIC}$ ($\Delta\delta^{13}C_{DIC}$) from the initial value for all the mesocosms. Most observations are clustered within the fourth quadrant, reflecting the natural prevalence of the degradation process within these mesocosms during the course of the experiment (Fig. 4 (b)). The degradation process seems to be amplified in the case of periclase and hydrated lime-II under low pCO_2 and high pH conditions, triggered by higher A_T additions (+500 μmol kg^{-1}). These findings align with those of Ferderer et al. (2022), who reported a significant decrease in the picoeukaryotes abundance compared to the control, suggesting that such physicochemical conditions are detrimental for the biome. de Castro et al. (2025) also studied the response of phytoplankton to ocean liming and reported a decrease in phytoplankton growth, but no overall changes in the community composition. While isotopic signatures and the DIC concentrations clearly reflect the amplified degradation process, additional data on changes in the phytoplankton abundance and biomass are needed to confirm these observations with greater confidence. The DIC and $\delta^{13}C_{DIC}$ data also reveal that no signature of

https://doi.org/10.5194/egusphere-2025-3925
Preprint. Discussion started: 26 August 2025

secondary precipitation was observed during the entire duration of the experiment. This again supplements our observations stated previously that the increase in $\Omega_{calcite}$ and $\Omega_{aragonite}$ due to the +A_T of both 250 and 500 μmol kg^{-1} for periclase and hydrated lime is insufficient to trigger the secondary precipitation, but is enough to cause substantial changes in A_T and pH. Hence, by enhancing A_T in a controlled manner, it is possible to increase the CO_2 sequestration potential of the ocean as well as buffer the ocean against acidification. The present study thus holds relevance not only towards the CDR research but also as a potential mitigation approach for ocean acidification. In addition, we provide a robust method for monitoring the secondary precipitation based on the temporal changes in the isotopic composition (δ^{13}C) of DIC along with the changes in the DIC concentration occurring within the mesocosms.

4.3 The northern Indian Ocean as a potential site for mCDR

Site selection also plays an important role in evaluating the OAE experiments, and various frameworks are being established to assess the sites and time for alkalinity release (Guo et al., 2025b). The northern Indian Ocean remains unexplored in terms of its potential for OAE as a mCDR method. It covers an area of 7×10^6 km^2, and surrounding the Indian subcontinent, features one of the longest coastlines (11×10^3 km). This extensive coastal ecosystem not only harbours marine biodiversity but could also emerge as a key potential site for implementing future CDR strategies owing to its socioeconomic benefits. There also exists a strong contrast in A_T between the Arabian Sea and the Bay of Bengal, driven mainly by the dilution in the latter due to large annual freshwater discharge, which may have a profound effect on changes in the $\Omega_{calcite}$ and $\Omega_{aragonite}$ due to mineral addition (Fig. 1 (a)). Through our experiment, we demonstrate the potential thresholds for alkalinity additions for periclase and hydrated lime. Owing to the heterogeneity of the coastal ecosystems, however, these thresholds might not be representative of the entire coastal Indian Ocean and may vary spatially. Hence, these thresholds must be applied with caution.

Nonetheless, this study provides a foundational understanding of the response of carbonate chemistry to alkalinity addition in the coastal ecosystem of the northern Indian Ocean in terms of OAE deployment, which has implications for advancing future CDR research. It offers valuable insights into the plausibility of the northern Indian Ocean as a potential site for implementing OAE in this region. In future scenarios, the assessment of deployment sites, the potential of different OAE methods and associated environmental impacts will play a crucial role in sustainable climate change mitigation (Vivian et al., 2025; Guo et al., 2025a; England and Bach, 2025).

Currently, a variety of OAE methods (alkalinity feedstocks) are being explored across different ecosystems, making it challenging to compare results globally. Therefore, it is essential to develop a standardised frameworks that allow OAE experiments using the same alkalinity feedstock to be conducted in different regions of the world, enabling more consistent and comparable assessments. OAEPIIP has been one of the initiatives to identify the response of phytoplankton communities to OAE across various global ecosystems (Bach et al., 2024). The findings from the present study may act as one of the many steps needed for such kind of assessments for effective CDR strategies.

https://doi.org/10.5194/egusphere-2025-3925
Preprint. Discussion started: 26 August 2025

5 Conclusions

In this study, we have evaluated the A_T generation potential of various alkalinity feedstocks at two different A_T levels in the coastal region of the southeastern Arabian Sea. Our results suggest that among all these minerals, periclase and hydrated lime cause a significant increase in A_T when dissolved in seawater. Contrary to this, naturally occurring minerals like olivine, dolomite and kaolinite did not show any dissolution, as overall no significant increase in A_T was observed. We further demonstrate that the secondary precipitation does not occur at +A_T of 250 and 500 μmol kg^{-1} for both periclase and hydrated lime. This indicates that these A_T perturbations of $\leq$500 μmol kg^{-1} can be considered safe thresholds for this region. However, it is possible that these thresholds might vary or may not be applicable along the entire coastal region. Hence, site-specific assessment of OAE will play an important role in determining these safe and effective limits. While the potential of olivine for OAE has been highlighted and discussed since the beginning of mCDR research, the study raises concerns regarding the effectiveness of olivine for OAE in the coastal region of the southeastern Arabian Sea, as no measurable changes in A_T were observed for both targeted levels. The isotopic data, coupled with the DIC, reveal enhanced remineralization during high pH and low pCO_2 conditions associated with higher A_T additions. These observations are helpful in establishing a baseline understanding of the response of the northern Indian Ocean to OAE and will further have important implications for guiding future CDR research in this region.

The baseline study captures the changes in the carbonate chemistry and various biogeochemical processes; however, more in situ experiments are required for a better assessment of the ecological and physiological response of OAE at multiple locations along the coastal regions of the Indian Ocean.

Data availability. All the data used in this study have been uploaded on Figshare and can be accessed through the following link: https://figshare.com/s/61ba34ee07f623113ee3

Author contributions. Experiment design and conceptualization - AS, execution of the experiment and sampling - SM, JK, SN, HS and IK, sample analysis - SM and JK, data analysis and interpretation - SM, JSR and AS, manuscript preparation - SM, manuscript editing and reviewing - SM and all co-authors, resources and funding - AS, SK, and IK

Competing interests. The contact author has declared that neither of the authors has any competing interests

Acknowledgements. We gratefully acknowledge A.K. Sudheer and Lennart Bach for their valuable suggestions on the chemical analysis of the samples. We also thank Tatsat Solanki for his assistance with mesocosm sampling. Our appreciation extends to Dwijesh Ray and Aditya

https://doi.org/10.5194/egusphere-2025-3925
Preprint. Discussion started: 26 August 2025

Das for conducting the XRD measurements, as well as to Sree Bhuvan Gandrapu for support with the XRF measurements. AS thanks the
300 DST-ANRF Swarnajayanti fellowship (SB/SJF/2021-22/11) for funding this work.

https://doi.org/10.5194/egusphere-2025-3925
Preprint. Discussion started: 26 August 2025

References

Bach, L. T.: The additionality problem of ocean alkalinity enhancement, Biogeosciences, 21, 261–277, https://doi.org/10.5194/bg-21-261-2024, 2024.

Bach, L. T., Ferderer, A. J., LaRoche, J., and Schulz, K. G.: Technical note: Ocean Alkalinity Enhancement Pelagic Impact Intercomparison Project (OAEPIIP), Biogeosciences, 21, 3665–3676, https://doi.org/10.5194/bg-21-3665-2024, 2024.

Bianchi, R., Abbate, S., Lockley, A., Abbà, A., Campo, F., Varliero, S., Grosso, M., and Caserini, S.: Evaluating rainbowing for ocean alkalinity enhancement, Environmental Research Communications, 6, 095 003, https://doi.org/10.1088/2515-7620/ad707b, 2024.

Burt, D. J., Fröb, F., and Ilyina, T.: The Sensitivity of the Marine Carbonate System to Regional Ocean Alkalinity Enhancement, Frontiers in Climate, 3, https://doi.org/10.3389/fclim.2021.624075, 2021.

Cannon, A. J.: Twelve months at 1.5 °C signals earlier than expected breach of Paris Agreement threshold, Nature Climate Change, 15, 266–269, https://doi.org/10.1038/s41558-025-02247-8, 2025.

de Castro, I., Ribeiro, S. C., Louvado, A., Gomes, N. C. M., Cachão, M., Brito de Azevedo, E., and Barcelos e Ramos, J.: Ocean liming effect on a North Atlantic microbial community: changes in composition and rates, Frontiers in Marine Science, 12, https://doi.org/10.3389/fmars.2025.1602158, 2025.

Dickson, A., Sabine, C., and Christian, J., eds.: Guide to Best Practices for Ocean CO Measurements, PICES Special Publication 3, North Pacific Marine Science Organization, available as a single PDF file, 2007.

Dickson, A. G.: Standard Potential of the Reaction: AgCl(s) + 1/2 H_2(g) = Ag(s) + HCl(aq) and the Standard Acidity Constant of the Ion HSO_4^- in Synthetic Sea Water from 273.15 to 318.15 K, The Journal of Chemical Thermodynamics, 22, 113–127, https://doi.org/10.1016/0021-9614(90)90074-Z, 1990.

Doney, S. C., Wolfe, W. H., McKee, D. C., and Fuhrman, J. G.: The Science, Engineering, and Validation of Marine Carbon Dioxide Removal and Storage, Annual Review of Marine Science, 17, 55–81, https://doi.org/10.1146/annurev-marine-040523-014702, 2025.

England, P. I. and Bach, L. T.: Influence of Wave Action on Applications of Olivine-Based Ocean Alkalinity Enhancement on Sandy Beaches, Geophysical Research Letters, 52, e2025GL114 922, https://doi.org/10.1029/2025GL114922, 2025.

Feely, R. A., Sabine, C. L., Lee, K., Berelson, W., Kleypas, J., Fabry, V. J., and Millero, F. J.: Impact of Anthropogenic CO2 on the CaCO3 System in the Oceans, Science, 305, 362–366, https://doi.org/10.1126/science.1097329, 2004.

Feng, E. Y., Keller, D. P., Koeve, W., and Oschlies, A.: Could artificial ocean alkalinization protect tropical coral ecosystems from ocean acidification?, Environmental Research Letters, 11, 074 008, https://doi.org/10.1088/1748-9326/11/7/074008, 2016.

Ferderer, A., Chase, Z., Kennedy, F., Schulz, K. G., and Bach, L. T.: Assessing the influence of ocean alkalinity enhancement on a coastal phytoplankton community, Biogeosciences, 19, 5375–5399, https://doi.org/10.5194/bg-19-5375-2022, 2022.

Ferderer, A., Schulz, K. G., Riebesell, U., Baker, K. G., Chase, Z., and Bach, L. T.: Investigating the effect of silicate- and calcium-based ocean alkalinity enhancement on diatom silicification, Biogeosciences, 21, 2777–2794, https://doi.org/10.5194/bg-21-2777-2024, 2024.

Foteinis, S., Andresen, J., Campo, F., Caserini, S., and Renforth, P.: Life cycle assessment of ocean liming for carbon dioxide removal from the atmosphere, Journal of Cleaner Production, 370, 133 309, https://doi.org/10.1016/j.jclepro.2022.133309, 2022.

Friedlingstein, P., O'Sullivan, M., Jones, M. W., Andrew, R. M., Hauck, J., Landschützer, P., Le Quéré, C., Li, H., Luijkx, I. T., Olsen, A., Peters, G. P., Peters, W., Pongratz, J., Schwingshackl, C., Sitch, S., Canadell, J. G., Ciais, P., Jackson, R. B., Alin, S. R., Arneth, A., Arora, V., Bates, N. R., Becker, M., Bellouin, N., Berghoff, C. F., Bittig, H. C., Bopp, L., Cadule, P., Campbell, K., Chamberlain, M. A., Chandra, N., Chevallier, F., Chini, L. P., Colligan, T., Decayeux, J., Djeutchouang, L. M., Dou, X., Duran Rojas, C., Enyo, K., Evans,

https://doi.org/10.5194/egusphere-2025-3925
Preprint. Discussion started: 26 August 2025

W., Fay, A. R., Feely, R. A., Ford, D. J., Foster, A., Gasser, T., Gehlen, M., Gkritzalis, T., Grassi, G., Gregor, L., Gruber, N., Gurses, O., Harris, I., Hefner, M., Heinke, J., Hurtt, G. C., Iida, Y., Ilyina, T., Jacobson, A. R., Jain, A. K., Jarnikova, T., Jersild, A., Jiang, F., Jin, Z., Kato, E., Keeling, R. F., Klein Goldewijk, K., Knauer, J., Korsbakken, J. I., Lan, X., Lauvset, S. K., Lefèvre, N., Liu, Z., Liu, J., Ma, L., Maksyutov, S., Marland, G., Mayot, N., McGuire, P. C., Metzl, N., Monacci, N. M., Morgan, E. J., Nakaoka, S.-I., Neill, C., Niwa, Y., Nützel, T., Olivier, L., Ono, T., Palmer, P. I., Pierrot, D., Qin, Z., Resplandy, L., Roobaert, A., Rosan, T. M., Rödenbeck, C., Schwinger, J., Smallman, T. L., Smith, S. M., Sospedra-Alfonso, R., Steinhoff, T., Sun, Q., Sutton, A. J., Séférian, R., Takao, S., Tatebe, H., Tian, H., Tilbrook, B., Torres, O., Tourigny, E., Tsujino, H., Tubiello, F., van der Werf, G., Wanninkhof, R., Wang, X., Yang, D., Yang, X., Yu, Z., Yuan, W., Yue, X., Zaehle, S., Zeng, N., and Zeng, J.: Global Carbon Budget 2024, Earth System Science Data, 17, 965–1039, https://doi.org/10.5194/essd-17-965-2025, 2025.

Geerts, L. J. J., Hylén, A., and Meysman, F. J. R.: The CDR potential of olivine-based enhanced rock weathering in marine systems: a case study for the coastal zone of France, Environmental Research Letters, 20, 074 049, https://doi.org/10.1088/1748-9326/addf60, 2025a.

Geerts, L. J. J., Hylén, A., and Meysman, F. J. R.: Review and syntheses: Ocean alkalinity enhancement and carbon dioxide removal through marine enhanced rock weathering using olivine, Biogeosciences, 22, 355–384, https://doi.org/10.5194/bg-22-355-2025, 2025b.

González, M. F. and Ilyina, T.: Impacts of artificial ocean alkalinization on the carbon cycle and climate in Earth system simulations, Geophysical Research Letters, 43, 6493–6502, https://doi.org/10.1002/2016GL068576, 2016.

Gruber, N., Bakker, D. C. E., DeVries, T., Gregor, L., Hauck, J., Landschützer, P., McKinley, G. A., and Müller, J. D.: Trends and variability in the ocean carbon sink, Nature Reviews Earth and Environment, 4, 119–134, https://doi.org/10.1038/s43017-022-00381-x, 2023.

Guo, J. A., Strzepek, R. F., Swadling, K. M., Townsend, A. T., and Bach, L. T.: Influence of ocean alkalinity enhancement with olivine or steel slag on a coastal plankton community in Tasmania, Biogeosciences, 21, 2335–2354, https://doi.org/10.5194/bg-21-2335-2024, 2024.

Guo, J. A., Strzepek, R. F., Yuan, Z., Swadling, K. M., Townsend, A. T., Achterberg, E. P., Browning, T. J., and Bach, L. T.: Effects of ocean alkalinity enhancement on plankton in the Equatorial Pacific, Communications Earth & Environment, 6, 270, https://doi.org/10.1038/s43247-025-02248-7, 2025a.

Guo, Y., Chen, K., Subhas, A. V., Rheuban, J. E., Wang, Z. A., McCorkle, D. C., Michel, A., and Kim, H. H.: Site selection for ocean alkalinity enhancement informed by passive tracer simulations, Communications Earth & Environment, 6, 535, https://doi.org/10.1038/s43247-025-02480-1, 2025b.

Hartmann, J., West, A. J., Renforth, P., Köhler, P., De La Rocha, C. L., Wolf-Gladrow, D. A., Dürr, H. H., and Scheffran, J.: Enhanced chemical weathering as a geoengineering strategy to reduce atmospheric carbon dioxide, supply nutrients, and mitigate ocean acidification, Reviews of Geophysics, 51, 113–149, https://doi.org/10.1002/rog.20004, 2013.

Hartmann, J., Suitner, N., Lim, C., Schneider, J., Marín-Samper, L., Arístegui, J., Renforth, P., Taucher, J., and Riebesell, U.: Stability of alkalinity in ocean alkalinity enhancement (OAE) approaches – consequences for durability of CO2 storage, Biogeosciences, 20, 781–802, https://doi.org/10.5194/bg-20-781-2023, 2023.

He, J. and Tyka, M. D.: Limits and CO2 equilibration of near-coast alkalinity enhancement, Biogeosciences, 20, 27–43, https://doi.org/10.5194/bg-20-27-2023, 2023.

Humphreys, M. P., Lewis, E. R., Sharp, J. D., and Pierrot, D.: PyCO2SYS v1.8: marine carbonate system calculations in Python, Geoscientific Model Development, 15, 15–43, https://doi.org/10.5194/gmd-15-15-2022, 2022.

Ilyina, T., Wolf-Gladrow, D., Munhoven, G., and Heinze, C.: Assessing the potential of calcium-based artificial ocean alkalinization to mitigate rising atmospheric CO2 and ocean acidification, Geophysical Research Letters, 40, 5909–5914, https://doi.org/10.1002/2013GL057981, 2013.

https://doi.org/10.5194/egusphere-2025-3925
Preprint. Discussion started: 26 August 2025

IPCC: Climate Change 2023: Synthesis Report. Contribution of Working Groups I, II and III to the Sixth Assessment Report of the Intergovernmental Panel on Climate Change, IPCC, Geneva, Switzerland, https://doi.org/10.59327/IPCC/AR6-9789291691647, 2023.

Keller, D. P., Feng, E. Y., and Oschlies, A.: Potential climate engineering effectiveness and side effects during a high carbon dioxide-emission scenario, Nature Communications, 5, 3304, https://doi.org/10.1038/ncomms4304, 2014.

Kheshgi, H. S.: Sequestering atmospheric carbon dioxide by increasing ocean alkalinity, Energy, 20, 915–922, https://doi.org/10.1016/0360-5442(95)00035-F, 1995.

Koishi, A.: Carbonate Mineral Nucleation Pathways, Ph.D. thesis, Université Grenoble Alpes, 2017.

Lan, X., Tans, P., and Thoning, K. W.: Trends in globally-averaged CO2 determined from NOAA Global Monitoring Laboratory measurements, https://doi.org/10.15138/9N0H-ZH07, version Thursday, 05-Jun-2025 08:00:43 MDT, 2025.

Lenton, A., Matear, R. J., Keller, D. P., Scott, V., and Vaughan, N. E.: Assessing carbon dioxide removal through global and regional ocean alkalinization under high and low emission pathways, Earth System Dynamics, 9, 339–357, https://doi.org/10.5194/esd-9-339-2018, 2018.

Lueker, T. J., Dickson, A. G., and Keeling, C. D.: Ocean pCO2 calculated from dissolved inorganic carbon, alkalinity, and equations for K1 and K2: validation based on laboratory measurements of CO2 in gas and seawater at equilibrium, Marine Chemistry, 70, 105–119, https://doi.org/10.1016/S0304-4203(00)00022-0, 2000.

Marín-Samper, L., Arístegui, J., Hernández-Hernández, N., Ortiz, J., Archer, S. D., Ludwig, A., and Riebesell, U.: Assessing the impact of CO2-equilibrated ocean alkalinity enhancement on microbial metabolic rates in an oligotrophic system, Biogeosciences, 21, 2859–2876, https://doi.org/10.5194/bg-21-2859-2024, 2024.

Minx, J. C., Lamb, W. F., Callaghan, M. W., Fuss, S., Hilaire, J., Creutzig, F., Amann, T., Beringer, T., Garcia, W. d. O., Hartmann, J., Khanna, T., Lenzi, D., Luderer, G., Nemet, G. F., Rogelj, J., Smith, P., Vicente, J. L. V., Wilcox, J., and Dominguez, M. d. M. Z.: Negative emissions—Part 1: Research landscape and synthesis, Environmental Research Letters, 13, 063 001, https://doi.org/10.1088/1748-9326/aabf9b, 2018.

Montserrat, F., Renforth, P., Hartmann, J., Leermakers, M., Knops, P., and Meysman, F. J. R.: Olivine Dissolution in Seawater: Implications for CO2 Sequestration through Enhanced Weathering in Coastal Environments, Environmental Science & Technology, 51, 3960–3972, https://doi.org/10.1021/acs.est.6b05942, 2017.

Moras, C. A., Bach, L. T., Cyronak, T., Joannes-Boyau, R., and Schulz, K. G.: Ocean alkalinity enhancement – avoiding runaway CaCO3 precipitation during quick and hydrated lime dissolution, Biogeosciences, 19, 3537–3557, https://doi.org/10.5194/bg-19-3537-2022, 2022.

NASEM: Negative Emissions Technologies and Reliable Sequestration: A Research Agenda, National Academies Press, Washington, D.C., ISBN 978-0-309-48452-7, https://doi.org/10.17226/25259, 2019.

NASEM: A Research Strategy for Ocean-based Carbon Dioxide Removal and Sequestration, National Academies Press, Washington, DC, ISBN 978-0-309-08761-2, http://www.ncbi.nlm.nih.gov/books/NBK580045/, copyright 2022 by the National Academy of Sciences. All rights reserved., 2021.

Oschlies, A., Bach, L. T., Fennel, K., Gattuso, J.-P., and Mengis, N.: Perspectives and challenges of marine carbon dioxide removal, Frontiers in Climate, 6, https://doi.org/10.3389/fclim.2024.1506181, 2025.

Paul, A. J., Haunost, M., Goldenberg, S. U., Hartmann, J., Sánchez, N., Schneider, J., Suitner, N., and Riebesell, U.: Ocean alkalinity enhancement in an open-ocean ecosystem: biogeochemical responses and carbon storage durability, Biogeosciences, 22, 2749–2766, https://doi.org/10.5194/bg-22-2749-2025, 2025.

Ramasamy, M., Amann, T., and Moosdorf, N.: Regional potential of coastal ocean alkalinization with olivine within 100 years, Environmental Research Letters, 19, 064 030, https://doi.org/10.1088/1748-9326/ad4664, 2024.

https://doi.org/10.5194/egusphere-2025-3925
Preprint. Discussion started: 26 August 2025

Rau, G. H., McLeod, E. L., and Hoegh-Guldberg, O.: The need for new ocean conservation strategies in a high-carbon dioxide world, Nature Climate Change, 2, 720–724, https://doi.org/10.1038/nclimate1555, 2012.

Renforth, P. and Henderson, G.: Assessing ocean alkalinity for carbon sequestration, Reviews of Geophysics, 55, 636–674, https://doi.org/10.1002/2016RG000533, 2017.

Riebesell, U., Basso, D., Geilert, S., Dale, A. W., and Kreuzburg, M.: Mesocosm experiments in ocean alkalinity enhancement research, State of the Planet, 2-oae2023, 1–14, https://doi.org/10.5194/sp-2-oae2023-6-2023, 2023.

Rohde, R.: Global Temperature Report for 2024, https://berkeleyearth.org/global-temperature-report-for-2024/, 2025.

Schuiling, R. D. and Krijgsman, P.: Enhanced Weathering: An Effective and Cheap Tool to Sequester Co2, Climatic Change, 74, 349–354, https://doi.org/10.1007/s10584-005-3485-y, 2006.

Simpson, G.: Comparing smooths in factor-smooth interactions II, From the Bottom of the Heap, https://www.fromthebottomoftheheap.net/2017/12/14/difference-splines-ii/, 2017.

Suessle, P., Taucher, J., Goldenberg, S. U., Baumann, M., Spilling, K., Noche-Ferreira, A., Vanharanta, M., and Riebesell, U.: Particle fluxes by subtropical pelagic communities under ocean alkalinity enhancement, Biogeosciences, 22, 71–86, https://doi.org/10.5194/bg-22-71-2025, 2025.

Suitner, N., Faucher, G., Lim, C., Schneider, J., Moras, C. A., Riebesell, U., and Hartmann, J.: Ocean alkalinity enhancement approaches and the predictability of runaway precipitation processes: results of an experimental study to determine critical alkalinity ranges for safe and sustainable application scenarios, Biogeosciences, 21, 4587–4604, https://doi.org/10.5194/bg-21-4587-2024, 2024.

Takahashi, T., Sutherland, S. C., Chipman, D. W., Goddard, J. G., Ho, C., Newberger, T., Sweeney, C., and Munro, D. R.: Climatological distributions of pH, pCO2, total CO2, alkalinity, and CaCO3 saturation in the global surface ocean, and temporal changes at selected locations, Marine Chemistry, 164, 95–125, https://doi.org/10.1016/j.marchem.2014.06.004, 2014.

Uppström, L. R.: The boron/chlorinity ratio of deep-sea water from the Pacific Ocean, Deep Sea Research and Oceanographic Abstracts, 21, 161–162, https://doi.org/10.1016/0011-7471(74)90074-6, 1974.

Venegas, R. M., Acevedo, J., and Treml, E. A.: Three decades of ocean warming impacts on marine ecosystems: A review and perspective, Deep Sea Research Part II: Topical Studies in Oceanography, 212, 105 318, https://doi.org/10.1016/j.dsr2.2023.105318, 2023.

Vivian, C., Boettcher, M., Elliot, M., Mengis, N., Merk, C., Oschlies, A., Boyd, P., Lancaster, A., Corry, O., Sugiyama, M., and Gupta, A.: The State of the Science for Marine Carbon Dioxide Removal (mCDR) – A Scientific Summary for Policy-Makers, UNESCO, Paris, France, https://doi.org/10.5281/zenodo.15490406, 2025.